Available online at www.sciencedirect.com
SciVerse ScienceDirect
Ceramics International 38 (2012) 4263–4269
CERAMICS INTERNATIONAL
www.elsevier.com/locate/ceramint

Study on microstructure and abrasive wear behavior of sintered Al matrix composites

Ali Mazahery, Mohsen Ostad Shabani *

Hashtgerd Branch, Islamic Azad University, Hashtgerd, Iran

Received 8 December 2011; received in revised form 15 January 2012; accepted 1 February 2012
Available online 9 February 2012

Abstract

Abrasive wear behavior of $ZrSiO_4$ reinforced aluminum metal matrix composite has been investigated in the present research. In general, composites offer superior wear resistance as compared to the alloy irrespective of applied load and zircon particles volume fraction. During sliding wear of the composite, a layer is formed over the specimen surface, which strongly dictates the wear behavior of the materials. It is believed that these layers are formed due to formation of wear debris, transfer of materials from the counter surfaces and mixing of these materials on the contact surfaces. The wear sliding test disclosed that the weight loss of the composites decreases with increasing volume fraction of zircon particulates. The composite samples were examined by X-ray diffraction technique and scanning electron microscopy which confirm the uniform distribution of zircon particles through the matrix. The hardness of the composite was affected significantly by the amount of porosity and reinforcement phase as two dominant factors.

Keywords: Aluminum; Powder metallurgy; Dry sliding

1. Introduction

Aluminum alloys are increasingly being implemented for structural applications, particularly in aerospace and automotive industries, owing to their low density, high thermal conductivity and high specific strength, which leads to the weight reduction resulting in a considerable economic advantage [1–8]. However, their low hardness and poor wear resistance are the main obstacles for their high performance tribological applications. During the last decades, enormous researches focusing on hard ceramic particulates, fibers, and whiskers reinforced aluminum metal matrix composites (AMMCs) have been performed due to modified specific strength, stiffness, wear resistance, fatigue resistance and elevated temperature applications, compared with conventional aluminum alloys [9–15].

The optimum properties of metal matrix composites (MMCs) and enhanced performance from these materials depend on a judicious selection of the reinforcing phase and the processing technique/parameters. Among the reinforcements such as SiC, B_4C, Al_2O_3, TiC and AlN zircon is the widely used due to the significantly high chemical stability and energy required for its reduction into zirconia and zirconium metal [16–19].

There are several manufacturing techniques for particle reinforced MMCs such as liquid metal infiltration, spray decomposition, squeeze casting, compocasting, powder metallurgy and mechanical alloying. Stir casting of MMCs is an attractive processing method for these advanced materials since it is relatively inexpensive, and offers a wide variety of material and processing condition options. Generally, these composites consist of a metal matrix, which is melted during casting, and ceramic reinforcement which is added to the molten matrix material by a mechanical stirrer [20]. In order to overcome some of the drawbacks associated with the conventional stir casting techniques, powder metallurgy (PM) techniques can be employed [21,22].

PM implies production of solid metallic materials and components from predominantly metallic powder. In principle, the microstructure of PM materials is similar to that of cast and wrought counterparts. There are, however, much more microstructural parameters, e.g., pore-related parameters, to

* Corresponding author. Tel.: +98 912 563 6709; fax: +98 261 6201888.
E-mail address: vahid_ostadshabany@yahoo.com (M.O. Shabani).

0272-8842/$36.00 © 2012 Elsevier Ltd and Techna Group S.r.l. All rights reserved.
doi:10.1016/j.ceramint.2012.02.008

be taken into account which are also relevant for mechanical and tribological behavior. Usually, the microstructure of PM materials is largely isotropic and texture-free, and powders and consolidated materials are virtually segregation-free. However, PM materials are sensitive to impurities (e.g., such as slag inclusions or foreign particles).

PM materials can principally be split up into two groups according to manufacturing route and resulting microstructure. PM precision parts are produced by cold uniaxial pressing and subsequent pressureless sintering (to some extent also by powder forging). The residual pores are usually regarded to be the principal characteristic. Fig. 1 shows schematically the main microstructural features occurring in PM materials. The most important parameters are total porosity and shape of pores/sintering contacts. Depending on total porosity which is influenced primarily by the compacting pressure and sintering conditions the sintering contacts can be isolated or interconnected. In the matrix, the larger microstructural flexibility of PM materials is significant, e.g., distribution of the alloy elements (both homogeneous and inhomogeneous) can be adjusted more freely than with ingot metallurgy.

PM full density products are made by hot isostatic pressing (e.g., PM superalloys and tool steels), by extrusion (PM aluminum alloys), or by pressing with subsequent liquid phase sintering (e.g., hard metals, tungsten heavy alloys, etc.). Residual porosity should be low to negligible, and the microstructure is commonly homogeneous. The most important feature affecting the behaviors and resulting in marked differences to cast or wrought counterparts is the usually very fine and isotropic microstructure which gives uniform properties regardless of the orientation. In contrast, the materials are sensitive to inclusions the effect of which is further aggravated by the excellent properties of the basic material. There have been researches on manufacturing the composites using the powder metallurgy methods. In addition, different properties of these composites affected by applied conditions have been investigated. Processing temperature, reinforcement fraction, particle size and the matrix strength are some of the factors studied and found out to be effective on the properties of the composites [23–25].

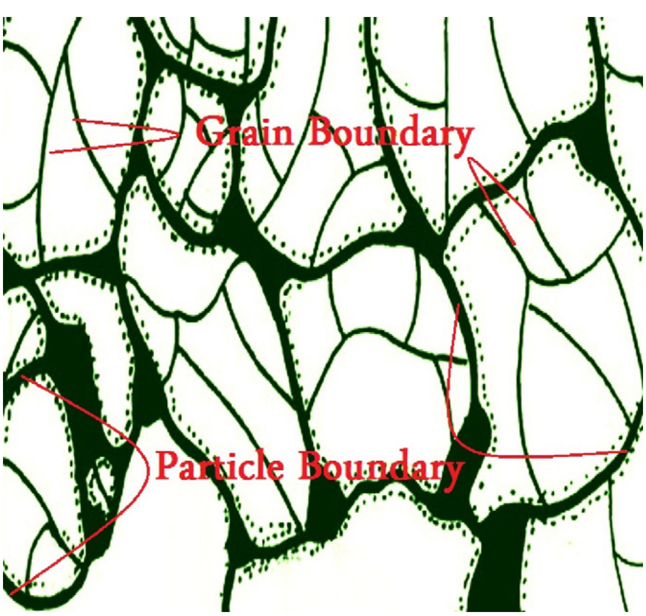

Fig. 1. Schematic microstructure of pressed and sintered PM material.

The enhancement in tribological properties of AMCs has been effectively attainable by introducing the ceramic particles. It has been generally observed that increasing the SiC or Al_2O_3 particle content enhances the wear resistance of the base alloy. The wear resistance of the composite was found to be considerably higher than that of the matrix alloy and increased with increasing particle content. The hard particles resist against destruction action of abrasive and protect the surface, so with increasing its content, the wear resistance enhances. This result is consistent with the rule that in general, materials with higher hardness have better wear and abrasive resistance [26–28]. In this study, zircon powders were incorporated into the Al matrix alloy using PM. In view of the above, sliding wear behavior of composites has been examined under varying applied loads and sliding distances.

2. Experimental procedure

The material analyzed in this work is the zircon particles reinforced aluminum matrix composite that is fabricated by a powder metallurgy process. In the first stage, different volume percentages of zircon (2.5, 5, 7.5, 10, 12.5, 15) with average particle size of 20 μm was added to aluminum powders (33 μm) by means of a planetary ball mill without protective atmosphere and with 1% zinc stearate applied as lubricant. The milling time and speed were 20 min and 600 rpm, respectively. In the next stage, the samples were compacted at Cold Isostatic Press (CIP) of 440 MPa and sintered at 600 °C under argon atmosphere for 65 min.

The samples were solution treated at 540 °C for 4 h, quenched into warm water (40 °C) and then peak aged to T6 condition (155 °C for 9 h). Microscopic investigations of the composite specimens and matrix alloy were carried out using a scanning electron microscope (SEM) (CAMSCAN-MV2300 Model, Oxford). In order to study the phase structure of the specimens, X-ray diffraction (XRD; Phillips PW-1800) was used. In addition, Brinell hardness values of the samples were measured on the polished samples using a ball with 2.5 mm diameter at a load of 31.25 kg. For each sample, five hardness tests on randomly selected regions were performed in order to eliminate the possible segregation effects and get a representative value of the matrix material hardness. During the hardness measurements, precaution was taken to make indentation at a distance of at least twice the diagonal length of the previous indention.

Sliding wear tests were conducted in pin-on-disk wear testing apparatus under varying applied loads against case hardened steel disk of hardness 63 HRC. Test specimens were cut and shaped in the form of pins having 6 mm in diameter and 25 mm in height. Before the abrasion tests, each specimen was polished to 0.5 μm. Fig. 2 shows schematic diagram of the abrasion wear test. The experiment was carried out at room

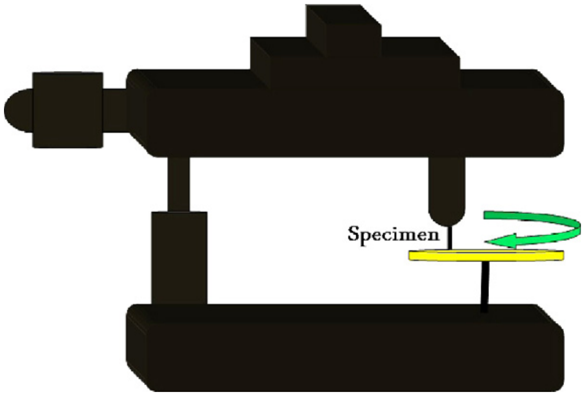

Fig. 2. Schematic diagram of the abrasion wear test.

temperature (21 °C, relative humidity 55%) with water as the lubricant. The samples were cleaned with acetone and weighed (up to an accuracy of 0.01 mg using microbalance) prior to and after each test. The temperature rise and friction force were recorded from the digital display interfaced with the wear test machine. Coefficient of friction was computed from the recorded frictional force and the applied load (i.e. the ratio of frictional force to the applied load). A set of three samples was tested in every experimental condition, and the average along with standard deviation for each set of three tests is measured. The wear tests were conducted up to the total sliding distance of 2000 m.

3. Results and discussion

X-ray diffraction was performed to determine the phase structure of the composites.

Fig. 3 shows the XRD pattern of the composite produced with 12.5 vol.% zircon. It can be seen that zircon and aluminum are present in the sample. The phases identified by XRD analysis were similar for all composites. These patterns show that zircon particles are incorporated into the aluminum matrix confirming that powder metallurgy method could be a rival to conventional methods like stir casting. The uniformity in distribution of particles within the sample is a microstructural feature which determines the in-service properties of particulate AMCs. In order to investigate the microstructure of composites, SEM micrographs were used. Because of difference between the densities of zircon and aluminum, the contrast of the micrographs is high enough for further study. Fig. 4 shows the micrographs of composites with 5 and 15 vol.% of zircon.

In these micrographs, the gray matrix is aluminum and the dispersed white spots represent aggregates of zircon particles. It can be seen that zircon particles are homogeneously dispersed throughout the composite sample. This uniform distribution of zircon particles can be attributed to appropriate time and method of mixing. Also there are some black points representing internal porosities of composites which are formed during powder metallurgy process. It can be observed that with increasing the zircon content of composites the

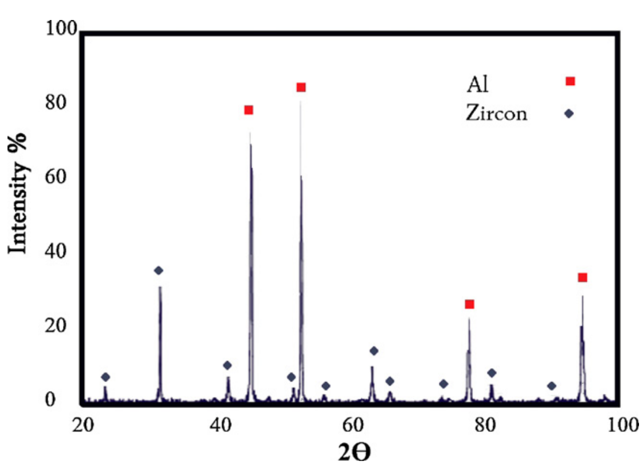

Fig. 3. XRD pattern of composite containing 12.5 vol.% zircon.

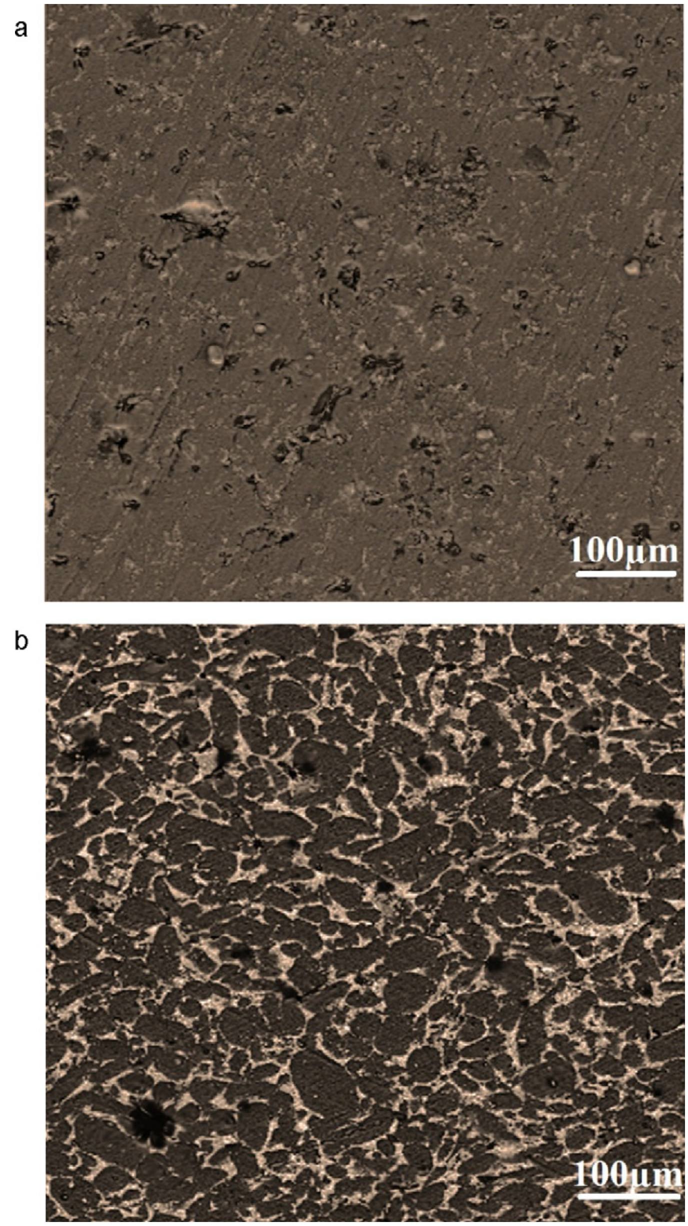

Fig. 4. SEM micrographs of composites: (a) 5 and (b) 15 vol.% zircon.

uniformity and homogeneity of specimens decrease and zircon clusters tend to segregate. Another phenomenon that can be clearly seen is that with increasing the zircon content of composites the amount of porosity is going up. This could be because of aggregation and clustering of zircon particles which prevent the densification of composites.

Generally, increasing porosities is a negative point in terms of mechanical behaviors as the discontinuity of the matrix phase will be higher and the stress concentration points will be more and more and these phenomena causes weak mechanical properties like strength. From another point of view, with addition of reinforcement particles, their random distribution changes and they agglomerate in some regions. These regions do not change during sintering. So they remain without any binding agent between them. In the higher volume percentages of zircon, these regions could be seen near every boundary. The direct contact of these zircon regions causes weak binding between boundaries; so the composite would not have the desired mechanical properties.

High temperature of sintering causes the easier diffusion of atoms which helps to increase the density of the composites. Clustering of zircon particles prevents the densification of composites. Agglomeration of zircon particles increases with the increase in volume fraction of zircon. Fig. 5 shows that increasing the zircon content resulted in the increase in the density of specimens. Relative density of the composite is defined as the ratio of the measured sintered density to theoretical density. This trend is increasing until 5% of zircon; after where there is a decreasing trend. This change in trends of composites is due to agglomeration of zircon particles during sintering process. It can be expected that in the sintering temperature, the zircon particles are totally dense with random distribution due to the high melting point of zircon. The dense network formed by zircon particles prevents the specimens to be dense [29].

Sliding wear is related to asperity-to-asperity contact of the two counter surfaces, which are in relative motion against each other. Fig. 6 shows the weight loss as a function of sliding distance at an applied load of 20 N. It is noted that the weight loss of the composites is less than that of unreinforced alloy,

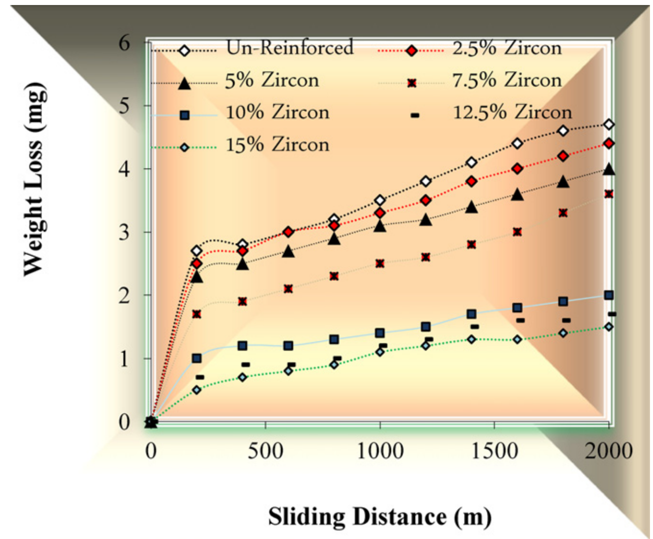

Fig. 6. Weight loss as a function of sliding distance.

increases with increase in sliding distance, and has a declining trend with increasing the particles volume fraction.

In general, composites offer superior wear as compared to the alloy irrespective of applied load and sliding speed. This result is consistent with the rule that in general, materials with higher hardness have better wear and abrasive resistance (Fig. 7).

At the initial stage of sliding, the wear is mainly due to fragmentation of asperities and removal of material due to cutting and flowing actions of penetrated hard asperities into the softer surface. Higher amount of stress is expected to act on the asperities, due to the greater degree of their hardness and sharpness. Because of the higher stress concentration on these points, they get plastically deformed and some of the sharpest asperities get fractured due to combined action of normal and shear stress. Fig. 8 represents the variation of temperature with sliding distance at an applied load of 25 N. During the sliding, in fact a considerable fraction of energy is spent on overcoming the frictional force, which leads to heating of the contact surfaces. Thus, it is expected that initially the temperature of the

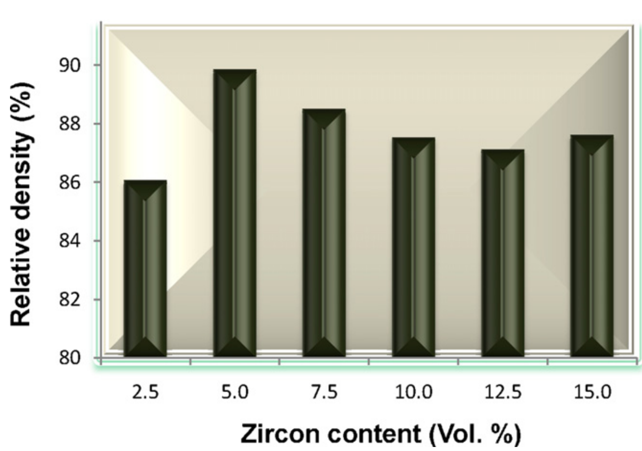

Fig. 5. Relative density of composites vs. zircon content.

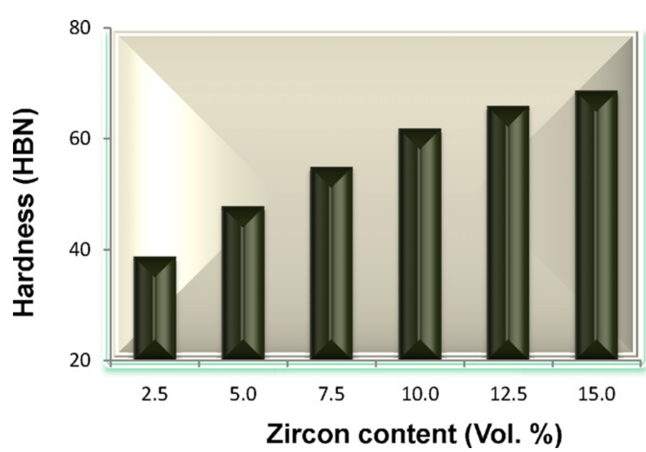

Fig. 7. Hardness as a function of zircon particles volume fraction.

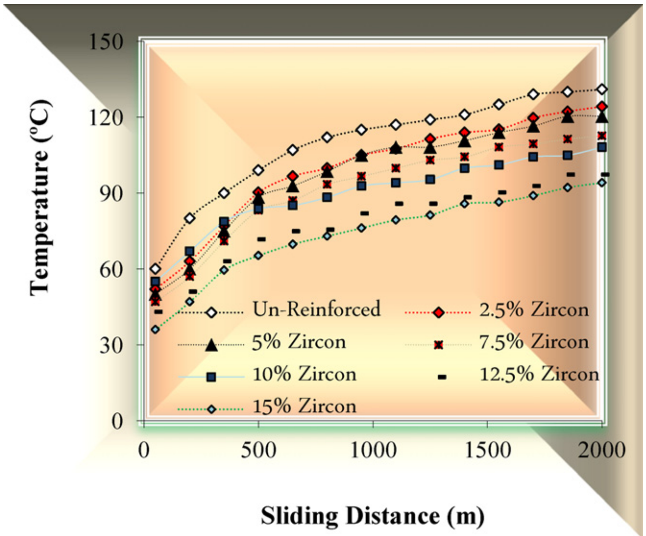

Fig. 8. Temperature as a function of sliding distance.

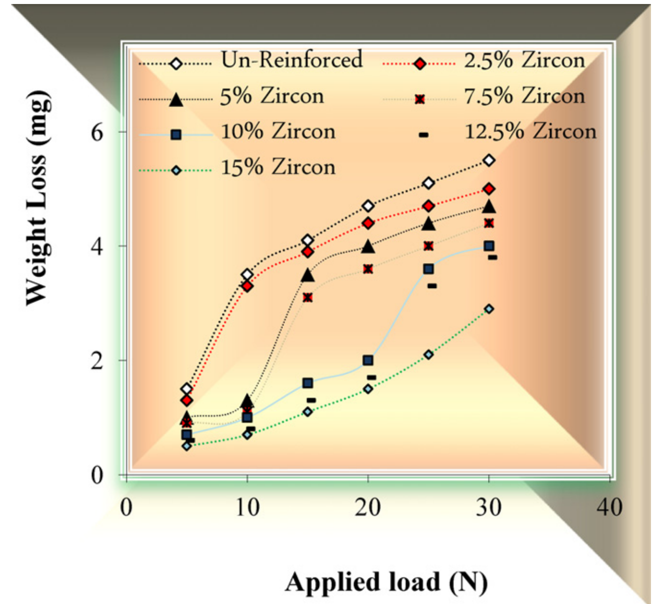

Fig. 9. Effect of applied load on wear resistance.

contact surface is less and hence the asperities are expected to be stronger and more rigid. As time progresses, the frictional heating increases, which leads to higher temperature and softening of the surface materials.

It is noted that temperature rise is greater in the case of unreinforced alloy as compared to that in the composite irrespective of the applied load and surface conditions. The rise in surfaces temperature is an outcome of a couple of facts that cause heating of the contact surfaces. During sliding, frictional force acts between the counter surfaces, which caused frictional heating of them. While the counter surfaces are in relative motion, the frictional heating is continuous because of insufficient time for heat dissipation. Initially, the asperities are stronger and sharper, and that is why frictional force and as a result frictional heating takes place at higher rate. After a certain period, because of the increase in flowability of the material on the specimen surface, slipping action is higher which results in reduction of frictional heating. The more possibility of adhesion between the counter surfaces leads to higher degree of friction. Because of these counter phenomena, frictional heating remains almost constant as observed in Fig. 8 [30,31].

It may be noted in Fig. 9 that the wear rate in all the samples increases marginally with applied load prior to reaching the critical load. The increase in the applied load leads to increase in the penetration of hard asperities of the counter surface to the softer pin surface. Beyond the critical load for each composite, the wear rate starts increasing abruptly with the applied load. The load at which wear rate increases suddenly to a very high value is termed as the transition load [32–34]. When the applied load is greater than the transition load, the wear rate of the composite shoots up to significantly higher value. This is attributed to the significantly higher frictional heating and thus the localized adhesion of the pin surface with the counter surface and also increase in softening of the surface material and thus more penetration of the asperities. Under such conditions the material removal due to the delamination of adhered areas, micro cutting and micro fracturing increases significantly [34,35].

The coefficient of friction is a composite function of the extent to which the energy is dissipated in the pin and the disk. Fig. 10 shows the changes in the friction coefficient (μ) with sliding distance. It can be seen that the friction coefficient of the composite specimen is lower than that of the unreinforced alloy. The coefficient of friction is related to the interaction of asperities between the counter surfaces, which in micro scale varies within specific range throughout the test period. This may result in fluctuation on friction coefficient within a narrow

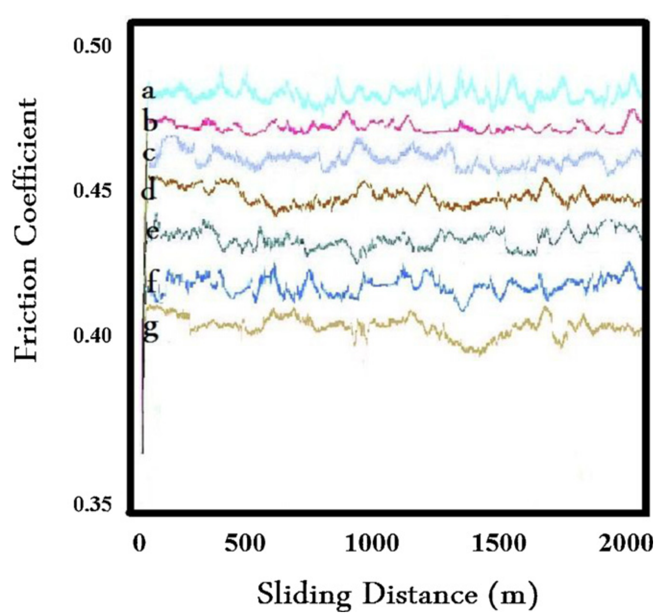

Fig. 10. Effect of sliding distance and particle sizes on friction coefficient (μ): (a) Unreinforced Al alloy; composites with zircon (b) 2.5 vol.%, (c) 5 vol.%, (d) 7.5 vol.%, (e) 10 vol.%, (f) 12.5 vol.%, (g) 15 vol.%.

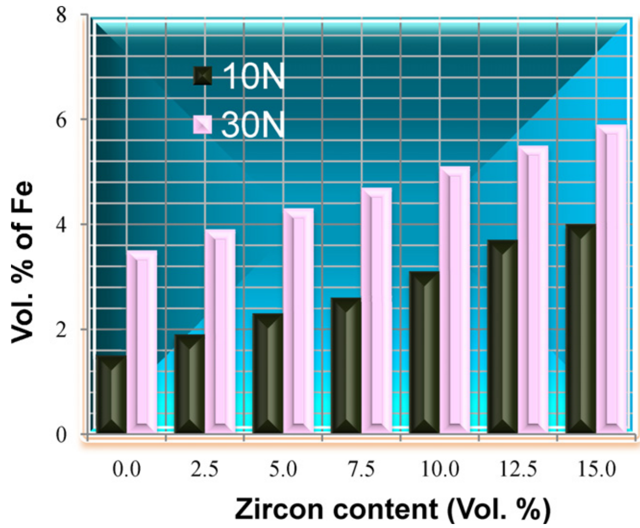

Fig. 11. Variations of the Fe content on the worn surface with zircon content.

range in each of the material with sliding distance. In the composite, the reinforcement particles support the load, so as to lessen the touch area between the pin and counter disk surface, decrease the friction coefficient and can prevent the scratch and cut from the surface [11,34]. This is probably one of the reasons for the observed enhancement in wear resistance of the composite. In addition, the higher formation of Fe rich layer on the worn surface may contribute to lower the coefficient of friction [12–14]. The formed layer on the worn surfaces of the pins is stable and substantially harder than the bulk material largely because it contains a fine mixture of Fe phase, Al and zircon. It is very likely that during the initial stages of sliding, the zircon particulates present in the composite pin plough into the steel disk and thus create a debris mostly containing iron. Iron may be present either as iron or as iron oxide. It is reported that iron might get oxidized during this process and oxide layers, in particular Fe_2O_3 layers generated during wear, act as solid lubricants and help to reduce the wear rates [35,31]. EDS analysis was used to detect the trace of Fe on the worn surfaces. Fig. 11 shows the Fe content variation on the worn surface with zircon content. It is observed that the formation of iron-rich layers on the contact surfaces increases with increasing the zircon content.

4. Conclusion

Combining aluminum and zircon will yield a material with the high wear resistance and mechanical properties. The microstructures of the composites were examined by scanning electron microscope in order to determine the distribution of the zircon particles and presence of porosity. It is observed that fabrication of these composites via PM technique lead to reasonably uniform distribution of particles in the matrix and minimum clustering or agglomeration of the reinforcing phase. The wear resistance of the composite was found to be considerably higher than that of the unreinforced alloy and increased with increasing particle content. The hard particles resist against destruction action of abrasive and protect the surface, so with increasing its content, the wear resistance enhances.

The wear rate in all the samples increases marginally with applied load prior to reaching the critical load. It is ascribed to the increase in fracture of reinforcement, the penetration of hard asperities of the counter surface into the softer pin surface and micro cracking tendency of the subsurface. After the critical load there is a transition from smooth linear increase wear rate to sudden increase in wear rate. This is attributed to the significantly higher frictional heating and thus the localized adhesion and softening of the surface with the counter surface. Coefficient of friction of the alloy and composites varies up and down within a narrow band with sliding distance. The friction coefficient of the composite specimen is seen to be lower than that of the unreinforced alloy.

References

[1] A. Mazahery, M.O. Shabani, Nano-sized silicon carbide reinforced commercial casting aluminum alloy matrix: experimental and novel modeling evaluation, Powder Technol. 217 (2012) 558–565.
[2] M.O. Shabani, A. Mazahery, Application of FEM and ANN in characterization of Al matrix nano composites using various training algorithms, Metall. Mater. Trans. A (2012), doi:10.1007/s11661-011-1040-1.
[3] A.M. Gokhale, G.R. Patel, Analysis of variability in tensile ductility of a semi-solid metal cast A356 Al-alloy, Mater. Sci. Eng. A 392 (2005) 184–190.
[4] X. Jian, H. Xu, T.T. Meek, Q. Han, Effect of power ultrasound on solidification of aluminum A356 alloy, Mater. Lett. 59 (2005) 190–193.
[5] X. Chen, H. Geng, Y. Li, Study on the eutectic modification level of Al–7Si alloy by computer aided recognition of thermal analysis cooling curves, Mater. Sci. Eng. A 419 (2006) 283–289.
[6] G. Heiberg, K. Nogita, A.K. Dahle, L. Arnberg, Columnar to equiaxed transition of eutectic in hypoeutectic aluminium–silicon alloys, Acta Mater. 50 (2002) 2537–2546.
[7] A. Mazahery, M.O. Shabani, Influence of the hard coated B4C particulates on wear resistance of Al–Cu alloys, Composites: Part B (2012), doi:10.1016/j.compositesb.2012.01.011.
[8] A. Mazahery, M.O. Shabani, Characterization of wear mechanisms in sintered Fe-1.5 Wt% Cu alloys, Arch. Metall. Mater. 57 (2012) 93–103.
[9] M.O. Shabani, A. Mazahery, Optimization of process conditions in casting aluminum matrix composites via interconnection of artificial neurons and progressive solutions, Ceram. Int. (2012), doi:10.1016/j.ceramint.2012.02.031.
[10] S. Chung, B.H. Hwang, A microstructural study of the wear behaviour of SiCp/Al composites, Tribol. Int. 27 (5) (1994) 307–314.
[11] A. Mazahery, M.O. Shabani, The accuracy of various training algorithms in tribological behavior modeling of A356–B4C composites, Russ. Metall. (Metall.) (2011) 699–707.
[12] M. Roy, B. Venkataraman, V.V. Bhanuprasad, Y.R. Mahajan, G. Sundararajan, Correlation between the characteristics of the mechanically mixed layer and wear behaviour of aluminium, Al-7075 Alloy and Al-MMCs, Metall. Trans. A 23 (1992) 2833–2846.
[13] S. Skolianos, T.Z. Kattamis, Tribological properties of SiC reinforced Al–4.5% Cu–1.5% Mg alloy composites, Mater. Sci. Eng. A 163 (1993) 107–113.
[14] M.K. Surappa, S.V. Prasad, P.K. Rohatgi, Wear and abrasion of cast Al-alumina particle composites, Wear 77 (1982) 295–302.
[15] A. Mazahery, M.O. Shabani, Investigation on mechanical properties of nano-Al_2O_3-reinforced aluminum matrix composites, J. Compos. Mater. 45 (2011) 2579–2586.
[16] P.V. Ananthapadmanabhan, K.P. Sreekumar, Influence of some process variables on plasma dissociation of zircon, Mater. Chem. Phys. 38 (1994) 15–20.

[17] R.C. Ewing, W. Lutze, Zircon: a host phase for the disposal of weapons plutonium, J. Mater. Res. 10 (1995) 243–246.
[18] A. Corradi, C. Leonelli, Effect of forming pressure on the reactivity and microstructure of zircon powder compacts, J. Mater. Sci. Lett. 12 (1993) 1434–1436.
[19] J. Ejiofor, B. Okorie, Powder processing and properties of zircon reinforced Al–13.5Si–2.5Mg alloy composites, J. Mater. Eng. Perform. 6 (1997) 326–334.
[20] A. Mazahery, M.O. Shabani, Tribological behaviour of semisolid–semisolid compocast Al–Si matrix composites reinforced with TiB_2 coated B4C particulates, Ceram. Int. (2011), doi:10.1016/j.ceramint.2011.10.016.
[21] A. Miserez, A. Mortensen, Fracture of aluminium reinforced with densely packed ceramic particles: influence of matrix hardening, Acta Mater. 52 (2004) 5331–5345.
[22] J. Torralba, C. da Costa, F. Velasco, P/M aluminum matrix composites: an overview, J. Mater. Process. Technol. 133 (2003) 203–206.
[23] H. Ferkel, B. Mordike, Magnesium strengthened by SiC nanoparticles, Mater. Sci. Eng. A 298 (2001) 193–199.
[24] A. Slipenyuk, V. Kuprin, The effect of matrix to reinforcement particle size ratio (PSR) on the microstructure and mechanical properties of a P/M processed AlCuMn/SiCp MMC, Mater. Sci. Eng. A 381 (2004) 165–170.
[25] M.O. Shabani, A. Mazahery, M.R. Rahimipour, M. Razavi, FEM and ANN investigation of A356 composites reinforced with B4C particulates, J. King Saud Univ. – Eng. Sci. (2011), doi:10.1016/j.jksues.2011.05.001.
[26] P.N. Bindumadhavan, H.K. Wah, O. Prabhakar, Dual particle size (DSP) composites: effect on wear and mechanical properties of particulate metal matrix composites, Wear 248 (2001) 112–120.
[27] J.K.M. Kwok, S.C. Lim, High-speed tribological properties of some Al/SiCp composites: II. Wear mechanisms, Compos. Sci. Technol. 59 (1999) 55–65.
[28] S. Das, D.P. Mondal, G. Dixit, Correlation of abrasive wear with microstructure and mechanical properties of pressure die-cast aluminum hard-particle composite, Metall. Mater. Trans. A 32 (2001) 633–642.
[29] Y.L. Shen, N. Chawla, On the correlation between hardness and tensile strength in particle reinforced metal matrix composites, Mater. Sci. Eng. A 297 (2001) 44–47.
[30] K. Konopka, M. Szafran, Fabrication of Al_2O_3–Al composites by infiltration method and their characteristic, J. Mater. Process. Technol. 175 (2006) 266–270.
[31] S.C. Lim, M.F. Ashby, Quantitative wear maps as a visualization of wear mechanism transitions in ceramic materials, Acta Metall. 35 (1987) 1–24.
[32] M.O. Shabani, A. Mazahery, Modeling of the wear behavior in A356–B4C composites, J. Mater. Sci. 46 (2011) 6700–6708.
[33] K. Razavizadeh, T.S. Tyre, Oxidative wear of aluminium alloys, Wear 79 (1982) 325–333;
S. Bueno, B. Ferrari, C. Melandri, G. de Portu, C. Baudín, Processing of aluminacoated tetragonal zirconia materials and their response to sliding, Ceram. Int. 38 (2010) 1545–1552.
[34] O.M. Shabani, A. Mazahery, Prediction of wear properties in A356 matrix composite reinforced with B4C particulates, Synth. Met. 161 (2011) 1226–1231.
[35] K.C. Ludema, A review of scuffing and running-in of lubricated surfaces, with asperities and oxides in perspective, Wear 100 (1984) 315–331.